Short communication

Opportunity of metallic interconnects for ITSOFC: Reactivity and electrical property

G. Cabouro [a,*], G. Caboche [a], S. Chevalier [a], P. Piccardo [b]

[a] *Laboratoire de Recherches sur la Réactivité des Solides, Université de Bourgogne, Dijon, France*
[b] *Università di Genova, Dipartimento di chimica e chimica industriale, Sezione di chimica inorganica e metallurgia, University of Genoa, Genoa, Italy*

Abstract

Iron-base alloys (Fe–Cr) are proposed hereafter as materials for interconnect of planar-type intermediate temperature solid oxide fuel cell (ITSOFC); they are an alternative solution instead of the use of ceramic interconnects. These steels form an oxide layer (chromia) which protects the interconnect from the exterior environment, but is an electrical insulator. One solution envisaged in this work is the deposition of a reactive element oxide coating, that slows down the formation of the oxide layer and that increases its electric conductivity. The oxide layer, formed at high temperature on the uncoated alloys, is mainly composed of chromia; it grows in accordance with the parabolic rate law ($k_p = 1.4 \times 10^{-12}$ g^2 cm^{-4} s^{-1}). On the reactive element oxide-coated alloy, the parabolic rate constant, k_p, decreases to 1.3×10^{-13} g^2 cm^{-4} s^{-1}. At 800 °C, the area-specific resistance of Fe–30Cr alloys is about 0.03 Ω cm^2 after 24 h in laboratory air under atmospheric pressure. The Y_2O_3 coating reduces the electrical resistance 10-fold. This indicates that the application of Y_2O_3 coatings on Fe–30Cr alloy allows to use it as an interconnect for SOFC.
© 2005 Elsevier B.V. All rights reserved.

Keywords: Chromia-forming alloy; Electrical resistivity; Oxidation; SOFC interconnect; MOCVD; Screen-printing

1. Introduction

The solid oxide fuel cell (SOFC) has evolved as one possibility of alternative energy. High-temperature SOFC have been investigated extensively as new electric power generating systems. This method of energy generation is still currently under investigation. The planar-type SOFC offers an attractive potential for increased power densities compared to other concepts. But the planar-type SOFC requires the application of an interconnect to join the anode of one cell to the cathode of the next cell in a voltage stack. It allows the distribution of anode and cathode gases as well as the transport of the electronic current between the individual cells and towards the external circuit. For these reasons, the interconnects are a major part of the SOFC components. Ceramic technology has been largely proposed as interconnects for SOFC working at high temperature (1000 °C). The decrease of the operating temperature in ITSOFC technology allows chromia-forming alloys to be used as interconnects. Using steel is cheaper; it includes the advantages of gas tight-

ness, machinability and high oxidation resistance as well as high mechanical strength.

For the fuel cell, the most commonly used materials are lanthanum strontium manganite (LSM) for the cathode, YSZ for the electrolyte and Ni–YSZ cermet for the anode. It is essential that the chosen interconnect material have the highest chemical stability, the highest oxidation resistance, as well as the highest electrical conductivity. Stainless steels may offer an interesting alternative to the ceramic interconnects. Advantageous properties of alloys are their gas tightness as well as their high oxidation resistance owing to the formation of Cr_2O_3 on their surface as a result of a selective oxidation of chromium. However, due to the high electrical resistance of this oxide layer, which is proportional to its thickness, the application of the above-mentioned alloys is possible only after some surface modifications. The main goal of this work was to study the oxidation behavior of uncoated and Y_2O_3-coated Fe–30Cr alloys during 24 h exposure in air under atmospheric pressure in the temperature range from 600 to 800 °C. The influence of this reactive element oxide on the thermally grown oxide layer electrical properties was also studied.

Y_2O_3 coatings were applied using the metal-organic chemical vapor deposition (MOCVD) technique. This reactive element

* Corresponding author.
E-mail address: Gwenael.Cabouro@u-bourgogne.fr (G. Cabouro).

Table 1
Fe–30Cr composition in wt.%

C	0.0021
Cr	29.95
S	0.0009
Fe	Balance

was chosen because previous studies showed that yttrium was more effective to improve the high temperature oxidation behavior of chromia-forming alloy [1,2]. Moreover many works have shown that the presence of yttrium modifies not only the oxide coating but also increases its electrical conductivity.

2. Experimental

2.1. Fe–30Cr (wt.%) alloy

The Fe–30Cr alloy is a laboratory made composition (Table 1). All the studied samples share the same cylindrical geometry (diameter: 10 mm, thickness: 1 mm). Fe–30Cr samples were ultrasonically degreased in alcohol, then submitted to an acid attack (in 1/3 HNO_3–2/3 H_2SO_4 mixture) in order to dissolve any metallic particles left over from the preparation process. They were then cleaned in distilled water and polished from 180-grit silicon carbide up to 1 μm with diamond paste, and finally cleaned in alcohol in an ultrasonic bath.

2.2. The MOCVD technique

Reactive element oxide coatings were prepared by MOCVD. A β-diketonate compound, the tris-2,2,6,6-tetramethyl-3,5-heptanedionato yttrium ($Y(tmhd)_3$) was used as the precursor; its synthesis was performed in the laboratory [3]. Coating conditions are summarized in Table 2.

The coating process has been described in detail elsewhere [4,5]. The reactive element oxide films were about 100 nm thick.

2.3. High temperature oxidation tests

The samples were oxidized for 24 h in laboratory air under atmospheric pressure; their oxidation was continuously monitored by thermogravimetry, using a thermobalance SETARAM TG 92. This microbalance measured a mass-variation at microgram scale. The oxidation tests were conducted at 600, 700, 800 and 850 °C, because these temperatures corresponded to the usual operating temperature range of ITSOFC.

Table 2
Coating conditions during the MOCVD process

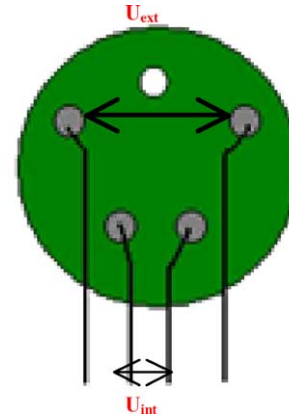|	Y_2O_3
Precursor temperature (°C)	170
Substrate temperature (°C)	600
N_2 flow rate (1 h^{-1})	7.5
O_2 flow rate (1 h^{-1})	2.5
Total pressure in reactor (mbar)	2

Fig. 1. Soldered electrodes on a sample (four-probe electrodes).

2.4. The electrical resistivity

The electrical resistivity measurements of the oxidized alloy were performed using a four-probe electrode during 24 h in air at 800 °C (Fig. 1).

The four-probe electrode was used because the measurement corresponded only to the oxide layer resistance. The electrode was soldered with platinum pastes on the sample surface. The samples were then placed directly into a furnace at a specific temperature. The furnace temperature was controlled by a thermocouple equipped EUROTERM 902. A Keithley 236 current source and a Keitley 2200 millimetric probe were used to measure the resulting voltage across the sample. The measurements were executed with a current of 0.3 A and with a voltage of 10 V.

Samples were pre-oxidized in laboratory air under atmospheric pressure during 24 h at 800 °C.

2.5. The ASR parameter

The area-specific resistance (ASR) parameter reflects the resistance, the thickness, as well as the electrical properties of the oxide layers. The calculation of the oxide-layer resistivity requires correct measurement of the thickness. It is generally accepted that the resistivity of the alloy substrate is negligible compared to that of the thermally grown oxide layer [6].

From the definition of the ASR parameters, Huang et al. [7] established a relation between the ASR and time t:

$$(ASR)^2 = \frac{(M_{Cr_2O_3})^2 k_p}{(3M_O \rho_{Cr_2O_3})^2 \sigma^2} \times t \quad (1)$$

where σ is the total conductivity of the oxide layer in S cm^{-1}, k_p the parabolic rate law constant, $M_{Cr_2O_3}$ and M_O the molar mass of chromia and of the oxygen, respectively, $\rho_{Cr_2O_3}$ the density of chromia and t the exposure time.

2.6. The screen-printing technique

The Fe–30Cr steel specimens were coated with an $La_{0.8}Sr_{0.2}MnO_3$ paste, using the screen-printing method. The paste was prepared by mixing in a closed system for 5 h an $La_{0.8}Sr_{0.2}MnO_3$ powder, a plasticizer and an organic binder.

The thickness of the deposited films was around 200 µm. The organic components were removed entirely from the paste during heating at 800 °C the coated specimens.

2.7. Characterization techniques

The oxidized surfaces were characterized using a scanning electron microscopy (SEM) with a field emission gun (FEG) coupled with an energy dispersive X-ray analysis (EDX).

3. Results

3.1. High temperature oxidation behavior of Y_2O_3-coated Fe–30Cr: oxidation kinetics

Fig. 1 shows the oxidation kinetics of the uncoated and Y_2O_3-coated samples at 800 °C in air. The comparison of the oxidation kinetics reveals that the mass gain of the coated alloy is four times lower than for the uncoated steel. The parabolic rate law constant, k_p, drastically decreases (one order of magnitude) (Fig. 2) on the coated steel.

3.2. Oxide layer characterization: influence of the reactive element

The oxide layer morphologies of the uncoated and Y_2O_3-coated samples were observed after a 24 h oxidation period at 800 °C in air under atmospheric pressure. This temperature was chosen because it is the maximum temperature in the temperature range used for ITSOFC.

The observed morphologies (Fig. 3) show that the oxide layer was different on the coated samples compared to that of the uncoated steels. The oxide layer grown on the uncoated sample exhibits micrometric and geometric grains made of chromia (Fig. 3a). The SEM image of the oxide layer formed on an Y_2O_3-coated sample shows very small grains of chromia (Fig. 3b). Moreover the yttria improves the oxidation resistance of the

(a)

(b)

Fig. 3. SEM image of the oxide layer after 24 h in air under atmospheric pressure at 800 °C: (a) surface of uncoated sample; (b) surface of Y_2O_3-coated sample.

sample, since the coating eliminates spallation and cavity formation between the metal and the oxide layer, whereas they are frequently observed on the uncoated alloy (Fig. 4a and b).

The SEM analyses of cross-sections (Fig. 5) show a decrease of the oxide layer thickness on the yttria-coated specimen. The oxide scale thickness is about 3 µm on the uncoated sample (Fig. 5a) and between 0.3 and 0.7 µm thick on the Y_2O_3-coated sample (Fig. 5b).

3.3. Electrical resistivity of oxide layer

The yttria coating influence on the metal conductivity was also studied. The yttria coating diminishes the value of the ASR parameter by a factor of 3 (Table 3) compared to the value obtained on an uncoated alloy.

The platinum influence was also controlled. Indeed, this element can perturb the oxidation [7]. The SEM image did not show any modification of the oxide layer morphology when Pt covered the surface. Indeed the middle of the oxide layer has
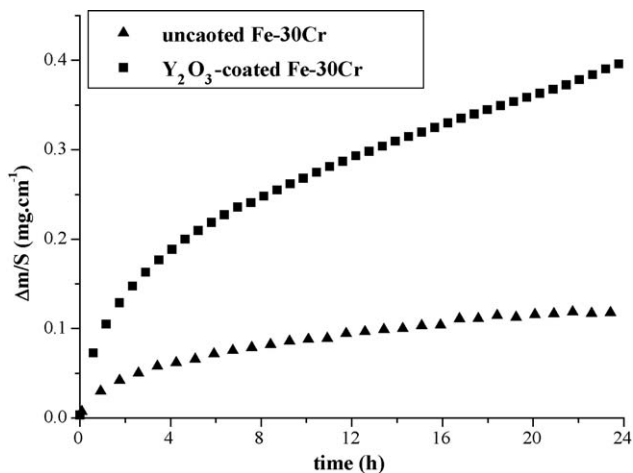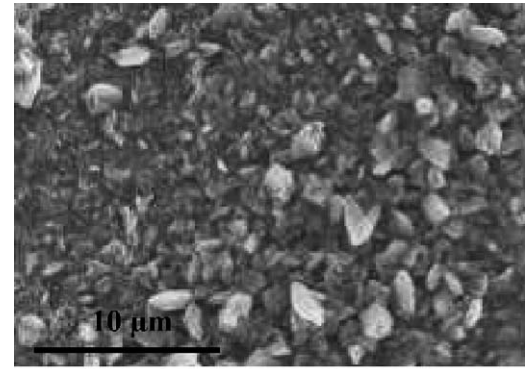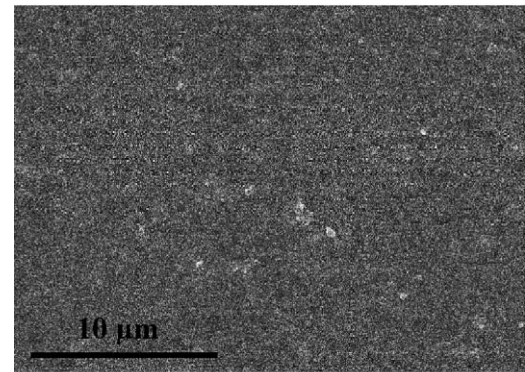

Fig. 2. High temperature oxidation kinetics of uncoated and Y_2O_3-coated samples during oxidation in laboratory air under atmospheric pressure (24 h at 800 °C).

Table 3
ASR values for in situ conductivity tests performed at 800 °C in air under atmospheric pressure during 24 h

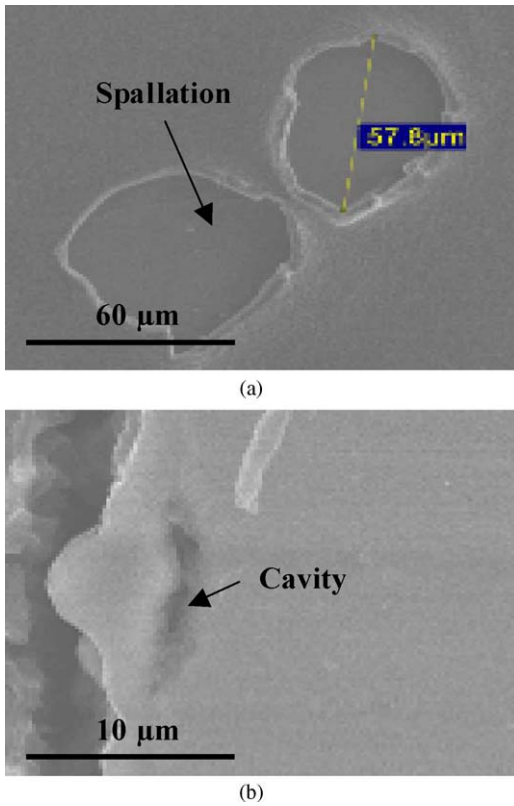|	Fe–30Cr pre-oxidized at 800 °C during 24 h	Fe–30Cr + Y_2O_3 pre-oxidized at 800 °C during 24 h
ASR (Ω cm^2)	3.2×10^{-2}	1.1×10^{-3}

Fig. 4. SEM cross-section image of chromia formed at 800 °C: (a) spallation on the oxide layer surface; (b) cavity between the metal and the oxide layer.
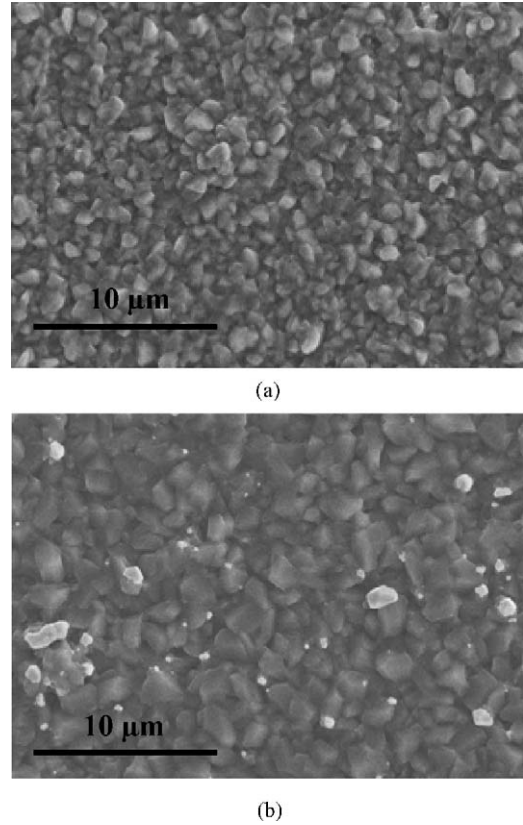
Fig. 6. SEM images of the oxide layer grown after in situ conductivity measurements at 800 °C during 24 h: (a) middle of the oxide layer; (b) oxide layer below the platinum solder.

the same morphology as the oxide layer under the platinum soldering (Fig. 6a and b). The oxide layer morphology after an in situ conductivity measurement is very close to the oxide layer morphology after oxidation in air at 800 °C during 24 h (Fig. 3a).

3.4. Metal/cathode interface characterization: influence of the reactive element

The influence of the yttria coating on the interface reactivity between a layer of lanthanum strontium manganite (LSM), which constitutes the cathode of the SOFC, and Fe–30Cr alloy was studied. Preliminary tests were made by applying a layer of about 200 μm thick of LSM.

The interface between the cathode material and the uncoated alloy exhibits a separation of the LSM layer (Fig. 7a). This separation does not exist at the interface between the LSM layer and the Y_2O_3-coated steel (Fig. 7b).

4. Discussion

For an oxidation carried out at 800 °C, the oxide layer of an uncoated sample is made of Cr_2O_3, which grows via cationic diffusion [8,9]. Cavities are formed at the metal/oxide layer interface owing to this growth process (Fig. 4b). These cavities may cause preferential detachments of the oxide layer [10]. The presence of extensive spallation (Fig. 4a) occurs after thermal stress release of the oxide layer during its cooling. This spallation and
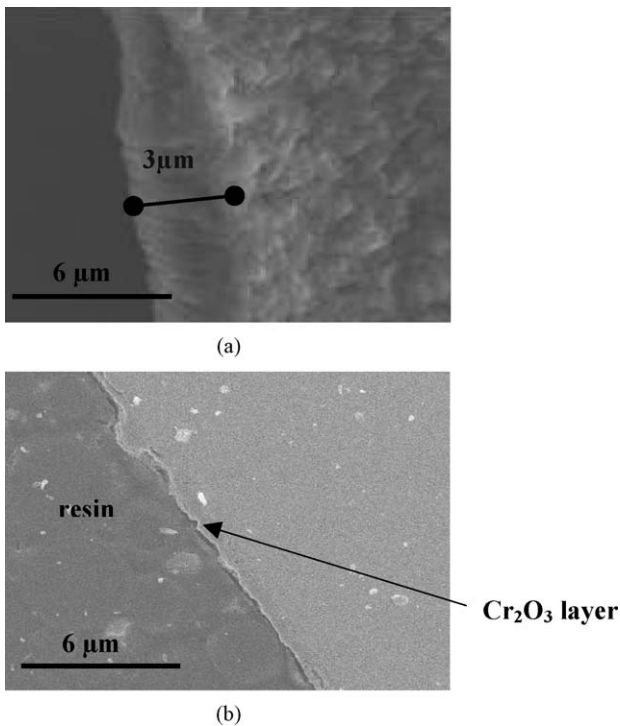

Fig. 5. SEM cross-section image of the oxide layer after 24 h in air under atmospheric pressure at 800 °C: (a) uncoated sample; (b) Y_2O_3-coated sample.
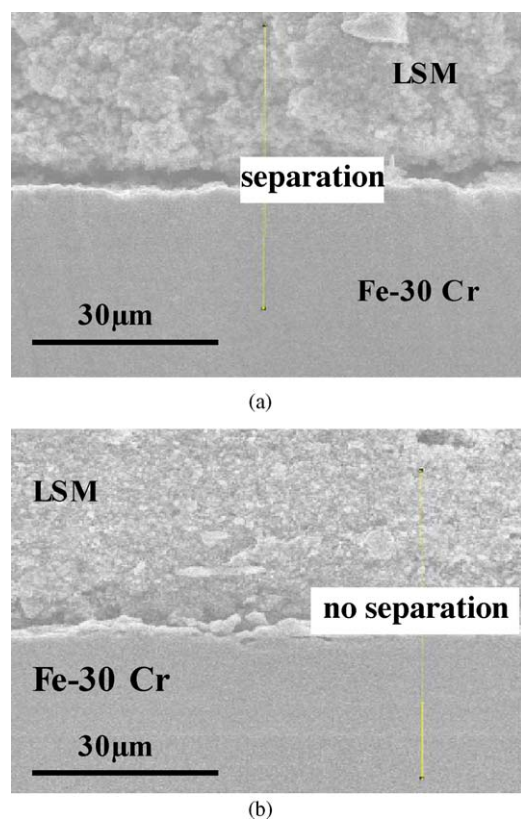
Fig. 7. SEM cross-section image showing the interface between LSM and the alloy after 24 h at 800 °C in air: (a) interface between LSM and Fe–30Cr; (b) interface between LSM and Y_2O_3-coated Fe–30Cr.

the presence of cavities are prejudicial defects for the use of this material as interconnects.

The study of the oxidation behavior of an Y_2O_3-coated alloy shows that this coating improves the property of the resultant oxide layer. In fact, it enables a decrease of the alloy mass-gain (four times) and of the parabolic rate law constant, k_p (10-fold), which is smaller than for the uncoated alloy (Fig. 2).

The oxide scale grown on the yttria-coated alloy is made of small equiaxed chromia grains (Fig. 3b). The dimension as well as the shape of the observed grains probably result from the segregation of the reactive elements towards the oxide grain boundaries [2]. On Y_2O_3-coated samples, no spallation is observed. In that case, stress is supposed to be relieved by plastic deformation of the chromia layer, owing to the modification of its grain morphology. Indeed, large columnar chromia grains grown on uncoated alloys and induce oxide layer failure during cooling to room temperature; whereas small equiaxed chromia grains develop on Y_2O_3-coated alloys, leading to stress without cracking. It is assumed that this modification of the chromia-layer plasticity is one of the main factors to improve the spallation resistance of alloys undergoing thermal shocks [11–14].

The elimination of spallation enables to consider the Y_2O_3-coated alloy as interconnects.

The electrical resistivity study shows that the yttria coating diminishes the value of the ASR parameter by a factor 3. It was also verified that the oxide layer morphology did not change

during the electrical test. The platinum did not seem to have any significant influence on the oxide layer development.

The ASR values were obtained after 24 h at 800 °C in air. In the literature, it is generally admitted that an alloy must have an ASR value below $0.1 \, \Omega \, cm^2$ to be able to be used as an interconnect [15,16]. The ASR value decrease observed in our case is encouraging at least after 24 h, but new coatings have to be considered (La_2O_3, Nd_2O_3, $LaCrO_3$, $NdCrO_3$, $YCrO_3$ coatings by MOCVD) in order to preserve this good conductivity, even after thousands hours in service conditions.

This work has been completed by the study of the interface reactivity between a layer of lanthanum strontium manganite (LSM), which constitutes the cathode of the SOFC, and the uncoated or Y_2O_3-coated alloy, in order to show that the yttria coating could improve the adherence of the cathode material on the selected interconnect material.

The interface reactivity study at high temperature between the cathode material and the uncoated or Y_2O_3-coated alloys enabled to show that the yttria coating improved the adherence of the LSM layer onto the metal (Fig. 7).

5. Conclusion

The initial objectives, which consist in choosing an interconnect material and in studying the high temperature oxidation behavior of this interconnect were reached. The application of an yttria coating by MOCVD, led to the improvement of the oxidation resistance by one order of magnitude, eliminating cavities and spallation, decreasing the oxidation rate as well as the chromia grain size.

Although the chromia is indispensable to protect the alloy, it is harmful to the compound electrical properties. In fact, chromia is an electrical insulator. Electrical measurement realized on Y_2O_3-coated samples showed a sharp decrease of the ASR parameter (by a factor 3).

In fact after 24 h at 800 °C in air under atmospheric pressure, the resistance of the yttria-coated alloy is of $1 \, m\Omega \, cm^2$. This decrease is sufficient to be efficient in a SOFC, since the generally accepted ASR value must be lower than $0.1 \, \Omega \, cm^2$.

References

[1] S. Chevalier, Ph.D. Thesis, Influence de dépôt MOCVD de Cr_2O_3 sur le comportement à haute température d'alliage chromino-formeur, Etude des mécanismes de réaction, University of Burgundy, Dijon, 1998.
[2] S. Chevalier, G. Bonnet, G. Borchardt, J.C. Colson, J.P. Larpin, Mechanisms involved by reactive elements upon high temperature chromia scale growth, Mater. Sci. Forum 327 (2001) 369.
[3] R.L. Burwell Jr., K. Schrage, Volatile rare earth chelates, J. Am. Chem. Soc. 87 (22) (1965) 5254.
[4] S. Chevalier, G. Bonnet, J.P. Larpin, Metal-organic chemical vapor deposition of Cr_2O_3 and Nd_2O_3 coatings. Oxide growth kinetics and characterization, Appl. Surf. Sci. 167 (2000) 125.

[5] S. Chevalier, G. Bonnet, J.C. Colson, J.P. Larpin, Influence of a reactive element oxide coating on the high temperature oxidation of chromia-former alloys, J. Chem. Phys. 95 (1998) 2083.

[6] K. Huang, P.Y. Hou, J.B. Goodenough, Characterization of iron-based alloy interconnects for reduced temperature solid oxide fuel cells, Solid State Ionics 129 (2000) 237.

[7] K. Huang, P.Y. Hou, J.B. Goodenough, Reduced area specific resistance for iron-base metallic interconnects by oxide coating, Mater. Res. Bull. 36 (2001) 81.

[8] S. Chevalier, G. Strehl, J. Favergeon, F. Desserrey, S. Weber, O. Heintz, G. Borchardt, J.P. Larpin, Use of oxygen isotopes to study transport mechanism during high temperature oxide scale growth, Mater. High Temp. 20 (2003) 253.

[9] R.E. Lobnig, H.P. Schnidt, K. Hennessen, H.J. Grabke, Diffusion of cations in chromia layers grown on iron-base alloys, Oxid. Met. 37 (1992) 81.

[10] P. Kofstad, High Temperature Corrosion, Elsevier Appied Science, New York, 1988.

[11] S. Chevalier, C. Valot, G. Bonnet, J.C. Colson, J.P. Larpin, The reactive element effect on thermally grown chromia residual stress, Mater. Sci. Eng. A 43 (2003) 257.

[12] A. Strawbridge, P.Y. Hou, The role of reactive elements in oxide scale adhesion, Mater. High Temp. 12 (1994) 177.

[13] P.Y. Hou, J. Stringer, The effect of reactive element additions on the selective oxidation, growth and adhesion of chromia scale, Mater. Sci. Eng. A 202 (1995) 1.

[14] S. Roure, F. Czerwinski, A. Petric, Influence of CeO_2 on the high temperature oxidation of chromium, Oxid. Met. 43 (1994) 75.

[15] K. Prybylski, T. Brylewski, J. Morgiel, Interfacial interaction between some La-based perovskite thick films and ferritic steel substrate with regard to the operating conditions of SOFC, Mater. Sci. Forum 461–464 (2004) 1099.

[16] W.Z. Zhu, S.C. Deevi, Opportunity of metallic interconnect for solid oxide fuel cells: a status on resistance, Mater. Res. Bull. 38 (2003) 957.